Instability modes of high-strength disclinations in nematics

D. Svenšek* and S. Žumer
Department of Physics, University of Ljubljana, Jadranska 19, SI-1000 Ljubljana, Slovenia
(Received 17 May 2004; revised manuscript received 10 August 2004; published 23 December 2004)

We solve the complete tensor fluctuation problem of a long and straight nematic disclination line with a general winding number in the one elastic constant approximation. Focusing on the eigenmodes growing in time, we show that the disclination with strength higher than $1/2$ is unstable with respect to the splitting and for integer strength also to the escape—in both cases there is no metastability. Numerically we show that a moderate elastic anisotropy, e.g., as found in thermotropic liquid crystals like 5CB or MBBA, does not introduce any metastability either.

DOI: 10.1103/PhysRevE.70.061707 PACS number(s): 61.30.Jf, 61.30.Dk, 47.15.Gf

I. INTRODUCTION

It is well known and apprehended that nematic disclination lines with winding numbers (strengths) higher than $1/2$ split into topological $1/2$ disclination lines, which can subsequently move apart reducing the free energy. The exact mechanism of the early stage of this splitting, however, has not been delivered, despite that one is interested in the nature of the perturbation leading to it. Moreover, the experimentally relevant question concerning the possible metastability of the high strength defect core with respect to the splitting has not been answered either. The situation is similar to the case of the escape in the third dimension, which is possible for disclinations with integer strengths. Here the instability issues were first addressed by Meyer [1] in 1973. As at that time the tensorial disclination structure had not been presented yet, a direct answer could not have been given.

In order to study the mechanism of the splitting and escape of the disclination, one must use the nematic tensor order parameter which provides a regular solution for the disclination core [2–4]. Even though the core may not be important macroscopically, e.g., energetically or in terms of observability, it is crucial for the stability of the defect structure. Therefore a special relevance of our study is in the aspect of connecting the macroscopic properties of the disclination to the microscopic, not directly observable properties of its core.

In this paper, using the one elastic constant approximation, we determine the exact tensor order parameter fluctuation eigenmodes of the disclination line with a general winding number. We search for the modes growing in time, which are responsible for the splitting and the escape. The effect of the elastic anisotropy on the instability against the splitting is studied numerically. Our results are particularly important in the context of the stability of planar radial structure in a capillary [5].

II. THE FLUCTUATION PROBLEM

We study the dynamics of perturbations of a long and straight nematic disclination line with a general winding number. Cylindrical coordinates (r,ϕ,z) with corresponding orthonormal base vectors $\{\hat{\mathbf{e}}_r,\hat{\mathbf{e}}_\phi,\hat{\mathbf{e}}_z\}$ will be used. The disclination line coincides with the z axis.

In the one elastic constant approximation, the free-energy density in terms of $\mathbf{Q}$ reads

$$f=\frac{1}{2}A\,\mathrm{Tr}\,\mathbf{Q}^2+\frac{1}{3}B\,\mathrm{Tr}\,\mathbf{Q}^3+\frac{1}{4}C(\mathrm{Tr}\,\mathbf{Q}^2)^2+\frac{1}{2}L\,\mathrm{Tr}(\boldsymbol{\nabla}\mathbf{Q}\cdot\boldsymbol{\nabla}\mathbf{Q}),\tag{1}$$

where in the last term the contraction over the gradient components is denoted by the dot. In this approximation, the free energy is invariant upon a homogeneous rotation of the $\mathbf{Q}$ tensor. This implies that the $\mathbf{Q}$ eigensystem rotates as $\psi=\psi_0+(s-1)\phi$ with respect to the above base vectors when we encircle a defect of strength s located at the origin; ψ is the angle between the director and $\hat{\mathbf{e}}_r$, and ψ_0 is the free parameter of the defect configuration corresponding to the angle between the director at $\phi=0$ and the x axis (e.g., for $+1$ defects $\psi_0=0$ represents the radial defect, while for the circular one $\psi_0=\pi/2$). There is no dependence on ϕ other than this rotation, i.e., the scalar invariants of $\mathbf{Q}$ (the degree of order and biaxiality) are independent of ϕ—a "generalized cylindrical symmetry." Let us define another orthonormal triad $\{\hat{\mathbf{e}}_1,\hat{\mathbf{e}}_2,\hat{\mathbf{e}}_z\}$,

$$\begin{bmatrix}\hat{\mathbf{e}}_1\\ \hat{\mathbf{e}}_2\end{bmatrix}=\begin{bmatrix}\cos\psi & \sin\psi\\ -\sin\psi & \cos\psi\end{bmatrix}\begin{bmatrix}\hat{\mathbf{e}}_r\\ \hat{\mathbf{e}}_\phi\end{bmatrix}.\tag{2}$$

With this, in the unperturbed configuration the $\mathbf{Q}$ tensor eigensystem coincides with the triad everywhere. We shall call this configuration the ground state, reminding that it should not carry the connotation of a state with minimal free energy. Further we define the five orthonormal symmetric traceless base tensors [6,7], Fig. 1,

$$\mathbf{T}_0=(3\hat{\mathbf{e}}_z\otimes\hat{\mathbf{e}}_z-\mathbf{I})/\sqrt{6},$$

$$\mathbf{T}_1=(\hat{\mathbf{e}}_1\otimes\hat{\mathbf{e}}_1-\hat{\mathbf{e}}_2\otimes\hat{\mathbf{e}}_2)/\sqrt{2},$$

$$\mathbf{T}_{-1}=(\hat{\mathbf{e}}_1\otimes\hat{\mathbf{e}}_2+\hat{\mathbf{e}}_2\otimes\hat{\mathbf{e}}_1)/\sqrt{2},$$

*Corresponding author. FAX: +386 1 2517281. Email address: daniel.svensek@fmf.uni-lj.si

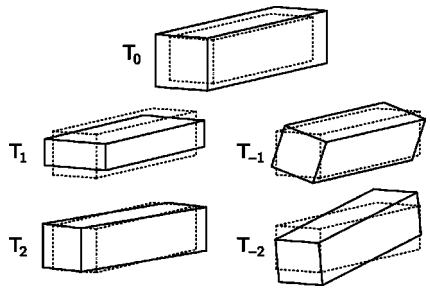

FIG. 1. Schematic representation of the perturbations described by the base tensors (3) for a uniaxial distribution with a positive degree of order (dashed). The **Q** tensor eigensystem is represented by the box, the length of the edges corresponds to the eigenvalue (plus a constant). $\mathbf{T}_0$ describes a perturbation of the degree of order, $\mathbf{T}_1$ describes a biaxial perturbation, $\mathbf{T}_{-1}$, $\mathbf{T}_2$, $\mathbf{T}_{-2}$ represent rotations of the eigensystem. The interpretation of the perturbations varies according to which of the axes has been identified with the director. Irrespective of this, the perturbations given by $\mathbf{T}_{-1}$, $\mathbf{T}_2$, and $\mathbf{T}_{-2}$ possess Goldstone modes, while those given by $\mathbf{T}_0$ and $\mathbf{T}_1$ are massive.

$$\mathbf{T}_2 = (\hat{\mathbf{e}}_z \otimes \hat{\mathbf{e}}_1 + \hat{\mathbf{e}}_1 \otimes \hat{\mathbf{e}}_z)/\sqrt{2},$$

$$\mathbf{T}_{-2} = (\hat{\mathbf{e}}_z \otimes \hat{\mathbf{e}}_2 + \hat{\mathbf{e}}_2 \otimes \hat{\mathbf{e}}_z)/\sqrt{2}, \tag{3}$$

with $\mathrm{Tr}(\mathbf{T}_i\mathbf{T}_j) = \delta_{ij}$. By virtue of the definition (2), the resulting eigenmode equations will be independent of ϕ and ψ_0, but will depend on the winding number s through spatial derivatives of the base tensors (3).

Expressing the **Q** tensor as

$$\mathbf{Q}(\mathbf{r},t) = q_i(\mathbf{r},t)\mathbf{T}_i(\mathbf{r}), \quad i = -2,-1,0,1,2, \tag{4}$$

and inserting it into Eq. (1) while being careful with the gradient $\boldsymbol{\nabla} = \hat{\mathbf{e}}_r\partial/\partial r + \hat{\mathbf{e}}_\phi\partial/r\partial\phi + \hat{\mathbf{e}}_z\partial/\partial z$ of the base tensors, f is expressed in terms of the tensor components q_i; the bulk (gradient-independent) part is

$$f^b = \frac{A}{2}q_i^2 + \frac{C}{4}(q_i^2)^2 + \frac{B}{18\sqrt{2}}\{9[q_1(q_2^2 - q_{-2}^2) + 2q_{-1}q_2q_{-2}] + \sqrt{3}q_0[2q_0^2 + 3(q_2^2 + q_{-2}^2 - 2q_1^2 - 2q_{-1}^2)]\} \tag{5}$$

and the elastic (gradient) part is

$$f^e = \frac{L}{2}\left\{\left(\frac{\partial q_i}{\partial r}\right)^2 + \left(\frac{\partial q_i}{\partial z}\right)^2 + \frac{1}{r^2}\left[\left(\frac{\partial q_0}{\partial \phi}\right)^2 + \left(\frac{\partial q_1}{\partial \phi} - 2sq_{-1}\right)^2 + \left(\frac{\partial q_{-1}}{\partial \phi} + 2sq_1\right)^2 + \left(\frac{\partial q_2}{\partial \phi} - sq_{-2}\right)^2 + \left(\frac{\partial q_{-2}}{\partial \phi} + sq_2\right)^2\right]\right\}. \tag{6}$$

We introduce dimensionless quantities: $r \to r/\xi$, $t \to t/\tau$, $(A,B,C) \to (A,B,C)\xi^2/L$, with the correlation length of the degree of order S (typically a few nm)

$$\xi = \sqrt{\frac{3}{2}\frac{L}{\left.\frac{d^2f}{dS^2}\right|_{S_0}}}, \tag{7}$$

where $\mathrm{Tr}\,\mathbf{Q}^2 = 3S^2/2$ (S_0 is the bulk equilibrium value of S), and the characteristic time (typically tens of ns)

$$\tau = \mu_1\xi^2/L, \tag{8}$$

where μ_1 is the bare rotational viscosity [8], i.e., $\gamma_1 = 9S^2\mu_1/2$; γ_1 is the usual director rotational viscosity. Neglecting the hydrodynamic flow, the order parameter dynamics is governed by the time-dependent Ginzburg-Landau equation, in the dimensionless form:

$$\dot{q}_i = \boldsymbol{\nabla}\cdot\frac{\partial f}{\partial\boldsymbol{\nabla}q_i} - \frac{\partial f}{\partial q_i} = \frac{\partial}{\partial r}\frac{\partial f}{\partial\frac{\partial q_i}{\partial r}} + \frac{1}{r}\frac{\partial f}{\partial\frac{\partial q_i}{\partial r}} + \frac{\partial}{r\partial\phi}\frac{\partial f}{\partial\frac{\partial q_i}{r\partial\phi}} + \frac{\partial}{\partial z}\frac{\partial f}{\partial\frac{\partial q_i}{\partial z}} - \frac{\partial f}{\partial q_i}, \tag{9}$$

where the time derivative vanishes in the ground state.

Owing to the generalized cylindrical symmetry, the ground state consists solely of the components q_0 and q_1, as opposed to perturbations where all the components are allowed. According to Eq. (9), the ground state components $q_0 = a_0$ and $q_1 = a_1$ satisfy

$$\frac{\partial^2 a_0}{\partial r^2} + \frac{1}{r}\frac{\partial a_0}{\partial r} - Aa_0 - \frac{1}{\sqrt{6}}B(a_0^2 - a_1^2) - C(a_0^2 + a_1^2)a_0 = 0, \tag{10}$$

$$\frac{\partial^2 a_1}{\partial r^2} + \frac{1}{r}\frac{\partial a_1}{\partial r} - \frac{4s^2}{r^2}a_1 - Aa_1 + \sqrt{\frac{2}{3}}Ba_0a_1 - C(a_0^2 + a_1^2)a_1 = 0 \tag{11}$$

and in the vicinity of $r = 0$ behave as

$$a_0 \approx c_0 + c_2r^2, \quad a_1 \approx br^{|2s|}, \tag{12}$$

with $c_2 = c_0(A + Bc_0/\sqrt{6} + Cc_0^2)/4$ and c_0, b extracted from the numerical solution in case they are needed. Asymptotically, due to the director distortion the ground state components behave as a power law rather than exponentially:

$$a_0 \to \frac{\sqrt{3}S_0}{2\sqrt{2}}\left[-1 + \frac{3s^2}{r^2}(1 + 1/g_1')\right],$$

$$a_1 \to \frac{3S_0}{2\sqrt{2}}\left[1 - \frac{3s^2}{r^2}(1 - 1/3g_1')\right], \tag{13}$$

where $g_1' = A - BS_0 + 3CS_0^2/2$. Putting

$$q_i(\mathbf{r},t) = \begin{cases} a_i(\mathbf{r}) + x_i(\mathbf{r},t), & i = 0,1 \\ x_i(\mathbf{r},t), & i = -1,2,-2, \end{cases} \tag{14}$$

where x_i are the perturbations, $x_i \ll a_{\{0,1\}}$, and linearizing Eqs. (9), one obtains two groups of coupled linear equations for the perturbations x_i:

$$\dot{x}_0 = \nabla^2 x_0 - g_0(r)x_0 + g_{01}(r)x_1, \tag{15}$$

$$\dot{x}_1 = \nabla^2 x_1 - \frac{4s^2}{r^2}x_1 - \frac{4s}{r^2}\frac{\partial x_{-1}}{\partial \phi} - g_1(r)x_1 + g_{01}(r)x_0, \tag{16}$$

$$\dot{x}_{-1} = \nabla^2 x_{-1} - \frac{4s^2}{r^2}x_{-1} + \frac{4s}{r^2}\frac{\partial x_1}{\partial \phi} - g_{-1}(r)x_{-1}, \tag{17}$$

and

$$\dot{x}_2 = \nabla^2 x_2 - \frac{s^2}{r^2}x_2 - \frac{2s}{r^2}\frac{\partial x_{-2}}{\partial \phi} - g_2(r)x_2, \tag{18}$$

$$\dot{x}_{-2} = \nabla^2 x_{-2} - \frac{s^2}{r^2}x_{-2} + \frac{2s}{r^2}\frac{\partial x_2}{\partial \phi} - g_{-2}(r)x_{-2}, \tag{19}$$

where $\nabla^2 x = \partial^2 x/\partial r^2 + 1/r\,\partial x/\partial r + \partial^2 x/r^2\partial\phi^2 + \partial^2 x/\partial z^2$ is the Laplacian in cylindrical coordinates and

$$g_0(r) = A + \sqrt{2/3}Ba_0 + C(3a_0^2 + a_1^2),$$

$$g_1(r) = A - \sqrt{2/3}Ba_0 + C(a_0^2 + 3a_1^2),$$

$$g_{-1}(r) = A - \sqrt{2/3}Ba_0 + C(a_0^2 + a_1^2),$$

$$g_{01}(r) = (\sqrt{2/3}B - 2Ca_0)a_1,$$

$$g_{\pm 2}(r) = A + B(a_0 \pm \sqrt{3}a_1)/\sqrt{6} + C(a_0^2 + a_1^2). \tag{20}$$

It is worth pointing out that defects with strengths s and $-s$ are formally equivalent, i.e., changing the sign of the defect and redefining $\mathbf{T}_{-1} \to -\mathbf{T}_{-1}$ and $\mathbf{T}_{-2} \to -\mathbf{T}_{-2}$ conserves the equations (15)–(20)—the sign of s in the equations is not changed.

III. FLUCTUATION MODES AND STABILITY

The eigensolutions of the systems (15)–(19) are sought by separation of variables using the ansatz (the global angular phase and the z phase are arbitrary)

$$\begin{Bmatrix} x_0 \\ x_1 \\ x_{-1} \end{Bmatrix} = \begin{Bmatrix} R_{0,m}(r)\cos(m\phi) \\ R_{1,m}(r)\cos(m\phi) \\ R_{-1,m}(r)\sin(m\phi) \end{Bmatrix} \sin(kz)\exp(-\lambda t), \tag{21}$$

$$\begin{Bmatrix} x_2 \\ x_{-2} \end{Bmatrix} = \begin{Bmatrix} R_{2,n}(r)\cos(n\phi) \\ R_{-2,n}(r)\sin(n\phi) \end{Bmatrix} \sin(kz)\exp(-\lambda t), \tag{22}$$

where m is an integer, whereas n is an integer if the strength s is an integer, and a half integer $n = 1/2, 3/2, 5/2, \ldots$ if s is a half-integer; this is due to the continuity and differentiability requirements (spinor symmetry of the base tensors). In the one elastic constant approximation, the sets of components (21) and (22) are not coupled, i.e., in-plane and out-of-plane fluctuations are independent. Furthermore, the z dependence is fully decoupled, i.e., the eigenfunctions $R_i(r)$ do not depend on k and the cross-sectional structure of the disclination line is not affected by the z modulation. The eigenvalue λ (the inverse time constant) decomposes into

$$\lambda = \lambda_r + k^2, \tag{23}$$

where λ_r is the eigenvalue of the radial and angular part. This time we are not interested in the z dependence and will omit it from the equations for brevity. In either case, only eigenvalue systems for the radial functions $R_i(r)$ remain, where $\lambda_r = \lambda$ is the eigenvalue:

$$\nabla^2 R_{0,m} + \left(\lambda - g_0(r) - \frac{m^2}{r^2}\right)R_{0,m} + g_{01}(r)R_{1,m} = 0, \tag{24}$$

$$\nabla^2 R_{1,m} + \left(\lambda - g_1(r) - \frac{m^2 + 4s^2}{r^2}\right)R_{1,m} - \frac{4sm}{r^2}R_{-1,m} + g_{01}(r)R_{0,m} = 0, \tag{25}$$

$$\nabla^2 R_{-1,m} + \left(\lambda - g_{-1}(r) - \frac{m^2 + 4s^2}{r^2}\right)R_{-1,m} - \frac{4sm}{r^2}R_{1,m} = 0, \tag{26}$$

and

$$\nabla^2 R_{2,n} + \left(\lambda - g_2(r) - \frac{n^2 + s^2}{r^2}\right)R_{2,n} - \frac{2sn}{r^2}R_{-2,n} = 0, \tag{27}$$

$$\nabla^2 R_{-2,n} + \left(\lambda - g_{-2}(r) - \frac{n^2 + s^2}{r^2}\right)R_{-2,n} - \frac{2sn}{r^2}R_{2,n} = 0. \tag{28}$$

One notices that the function operators (15)–(19) are self-adjoint, possessing real eigenvalues and orthogonal eigenmodes. The eigensystems (24)–(28) are solved numerically. We use a multidimensional Newton relaxation method ([9], p. 588) or in some cases also a shooting method ([9], p. 588).

If $\lambda > 0$, the mode is decaying and the ground state is (meta)stable against the corresponding fluctuation. The most important family of modes with $\lambda > 0$ is generated from the Goldstone mode that corresponds to a homogeneous displacement of the disclination line. Modifying the displacement sinusoidally along z results in the stringlike fluctuations of the disclination line [10], which are the ones that can be observed, e.g., by polarization microscopy [11].

In the search for a splitting and/or escape instability, from now on we will focus our attention to possible growing modes, i.e., those for which $\lambda < 0$.

Due to the singularity of the cylindrical coordinates, the behavior of the ground state and the radial eigenfunctions near the origin must be determined analytically. In the shooting procedure, the unknown coefficients of the radial eigenfunction expansion have to be determined together with the eigenvalue λ. For numerical reasons, we restrict the eigenmodes to vanish at an arbitrary but not too large a value of $r = r_0$. This presents no problem as the modes concerned are localized (decaying exponentially with r, see below) and hence remain unaffected by the restriction if only one makes r_0 large enough compared to the characteristic decay length of the mode.

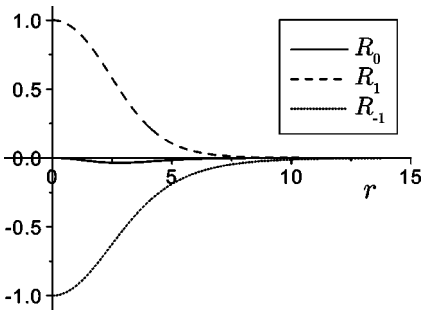

FIG. 2. Radial eigenfunctions of the splitting fluctuation, $s=1$, $m=2$, $\lambda=-0.22$. The length unit is $\xi=2.11$ nm, the time unit is $\tau=32.6$ ns. For comparison, the eigenvalue of the fastest escape mode is $\lambda=-0.0042$.

IV. SPLITTING MODES

The modes responsible for the splitting do not involve the components x_2 or x_{-2}, since the **Q** tensor eigensystem does not get rotated out of the xy plane in this process. Therefore the system (15)–(17) must be examined. The lowest-order expansion of the system (24)–(26) around the origin is

$$R_0 \approx r^m, \quad R_{\pm 1} \approx \begin{cases} \pm k_1 r^{|m-2s|} \\ k_2 r^{|m+2s|}, \end{cases} \tag{29}$$

where the two solutions for R_1 and R_{-1} are independent.

First we study the simplest case, i.e., the splitting of the ± 1 defect. Then we make a generalization to defects of other strengths. In the case of the splitting of the ± 1 defect to two $\pm 1/2$ defects, the modes in question must exhibit a quadrupolar symmetry, which sets $m=2$ in the angular part of Eq. (21). A single growing mode ($\lambda=-0.22$) is found (Figs. 2 and 3), which is localized to the core within a few correlation lengths, while all the others (including those with $m\neq 2$) are decaying and nonlocalized. Due to the localization, the growing mode cannot be affected by any confinement unless it comes down to the ξ scale—it is an intrinsic feature of the defect structure. It is no sooner than at a confinement of $r_0=3.5\xi$ that the mode becomes decaying.

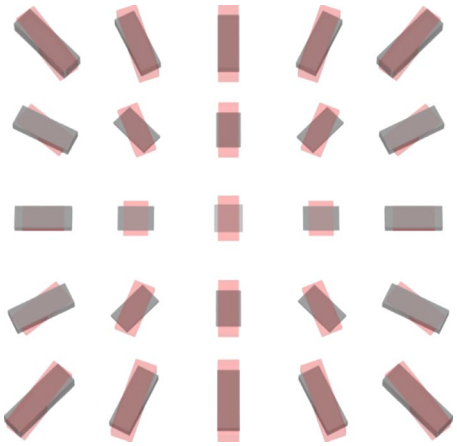

FIG. 3. (Color online) Cross section through the $s=1$ radial disclination line: the ground state (gray/dark) is perturbed by the splitting mode (red/light), leading to two $1/2$ disclinations on the x axis. Note the two uniaxial regions of the perturbed structure corresponding to the centers of the $1/2$ disclinations.

For any winding number, the radial functions are localized if and only if the mode is of the growing type, which can be seen from their behavior for $r \gg 1$:

$$R_{-1,m} \propto K_m(\sqrt{-\lambda}r), \tag{30}$$

$$R_{\{0,1\},m} \propto \frac{4ms}{r^2} R_{-1,m}, \tag{31}$$

where K_m is the modified Bessel function of the second kind with the asymptotics $K_m(x) \propto \exp(-x)/\sqrt{x}$. The modes with $\lambda<0$ have a discrete spectrum, whereas the spectrum of those with $\lambda>0$ is continuous for an infinite system.

It is instructive to study the influence of the hydrodynamic flow generated by the order parameter dynamics (the backflow) on the growth rate of the mode. This is performed numerically, where the coupling of the flow and **Q** tensor fields is described by the tensorial version of the Ericksen-Leslie theory [8]. The one elastic constant approximation is used, the numerical method and the material parameters are given in [12]. It is important to realize that the velocity field behaves quasistationary (adiabatic limit), i.e., the characteristic dynamic time of the velocity field is typically a million-times smaller than the characteristic dynamic time of the **Q** field. Therefore what is actually solved is the stationary Navier-Stokes equation (in the low-Reynolds-number and incompressibility limits). Hence the backflow does not bring in any inertial effects that would result in oscillatory modes. Furthermore, as the velocity field is an enslaved variable it does not represent an independent degree of freedom and as such does not introduce any new modes.

It is found that the backflow correction to the growth rate is small, i.e., less than 5%, speeding up the modes. The correction is expected to be small. In the region where the splitting mode is nonzero, **Q** (i.e., $\mathrm{Tr}\,\mathbf{Q}^2$) is small, but we know that the velocity of the backflow decreases with decreasing **Q** (that is, decreasing $\mathrm{Tr}\,\mathbf{Q}^2$), as does its influence on **Q**. At the same time one should be quite reserved, since the description of the flow to **Q** tensor coupling [8] is not complete and the missing terms [13] could play a noteworthy role in the dynamics of the defect core. Moreover, one must recall that the applicability of hydrodynamic equations is questionable at length and time scales that small (1 nm, 10 ns).

In the case of defects with higher strengths, there exists an increasing number of splitting modes as there are more and more ways the defect can split. It turns out that for every decomposition allowed topologically one can find at least one splitting mode, provided that none of the resulting winding numbers is too high. Each of these modes exhibits a distinctive angular symmetry set by its value of m. Generally, a defect of strength $\pm s$ splits to m symmetrically placed $\pm 1/2$ defects surrounding a $\pm s \mp m/2$ defect, which remains in the center (Fig. 4). For example, a possible splitting channel of a defect with strength 2 is $2 \rightarrow -1+6\times 1/2$, where the -1 defect stays in the middle, surrounded by the $1/2$ defects. The corresponding mode has a sixfold symmetry, $m=6$. On the other hand, this defect is stable with respect to the splitting

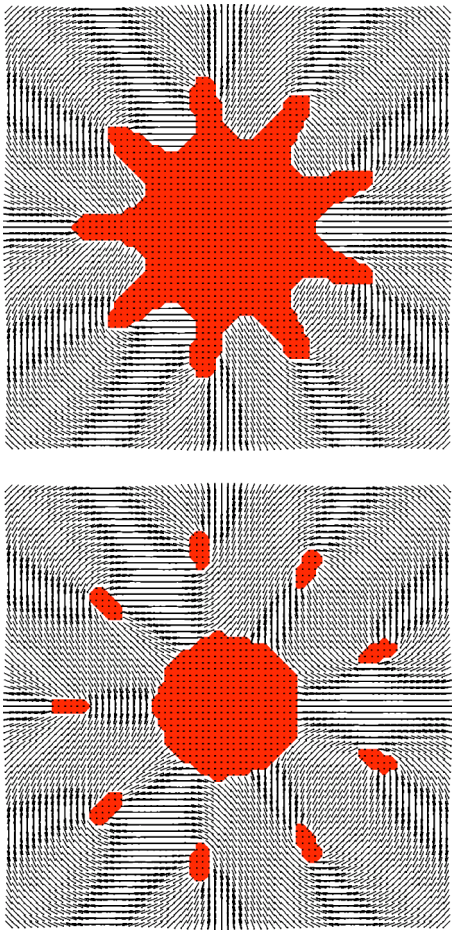

FIG. 4. A ninefold ($m=9$) splitting of the $s=3$ defect. The lower diagram depicts a $-3/2$ defect in the center and nine $1/2$ defects around it. The shading denotes regions of reduced degree of order.

$2\rightarrow -3/2+7\times 1/2$ and higher. All possible splitting channels of defects with strengths $\leqslant 3$ are given in Table I, the growth rates are plotted in Fig. 5. Learning from the results for $s\leqslant 3$, the splitting modes exist for $2\leqslant m\leqslant 2(2s-1)$; in other words, the winding number s' of the disclination remaining in the center is $(s-1)\geqslant s'\geqslant -(s-1)$. The splitting into $\pm 1/2$ defects only is always the fastest.

V. ESCAPE MODES

In an unconfined system, planar defects with integer strengths can escape to the undeformed configuration with a zero deformation free energy (escape in the third dimension) [14,1]. Equipped with the present formalism, we are able to look for another type of possibly growing modes leading to the escape. As here the **Q** tensor eigensystem is rotated out of the xy plane, the system (18) and (19) must be examined at this time. In particular, one expects the perturbation x_2 to be crucial, as it corresponds to the out-of-plane rotation of the director. The lowest-order expansion of the system (27) and (28) around the origin is

TABLE I. Fastest splitting modes with a given m for disclinations with $|s|\leqslant 3$. For negative winding numbers the situation is analogous.

Splitting	m	$-\lambda$
$1\rightarrow 2\times 1/2$	2	0.22
$3/2\rightarrow 1/2+2\times 1/2$	2	0.13
$3/2\rightarrow 3\times 1/2$	3	0.34
$3/2\rightarrow -1/2+4\times 1/2$	4	0.12
$2\rightarrow 1+2\times 1/2$	2	0.091
$2\rightarrow 1/2+3\times 1/2$	3	0.25
$2\rightarrow 4\times 1/2$	4	0.40
$2\rightarrow -1/2+5\times 1/2$	5	0.25
$2\rightarrow -1+6\times 1/2$	6	0.073
$5/2\rightarrow 3/2+2\times 1/2$	2	0.068
$5/2\rightarrow 1+3\times 1/2$	3	0.19
$5/2\rightarrow 1/2+4\times 1/2$	4	0.32
$5/2\rightarrow 5\times 1/2$	5	0.43
$5/2\rightarrow -1/2+6\times 1/2$	6	0.32
$5/2\rightarrow -1+7\times 1/2$	7	0.19
$5/2\rightarrow -3/2+8\times 1/2$	8	0.044
$3\rightarrow 2+2\times 1/2$	2	0.053
$3\rightarrow 3/2+3\times 1/2$	3	0.16
$3\rightarrow 1+4\times 1/2$	4	0.27
$3\rightarrow 1/2+5\times 1/2$	5	0.37
$3\rightarrow 6\times 1/2$	6	0.45
$3\rightarrow -1/2+7\times 1/2$	7	0.37
$3\rightarrow -1+8\times 1/2$	8	0.27
$3\rightarrow -3/2+9\times 1/2$	9	0.15
$3\rightarrow -2+10\times 1/2$	10	0.025

$$R_{\pm 2}\approx\begin{cases}\pm r^{|n-s|}\\ kr^{|n+s|};\end{cases} \tag{32}$$

k is determined together with the eigenvalue in the shooting procedure. For $n=0$, the equations (27) and (28) are decoupled. It is exactly in this case that one finds $\lambda<0$ and the

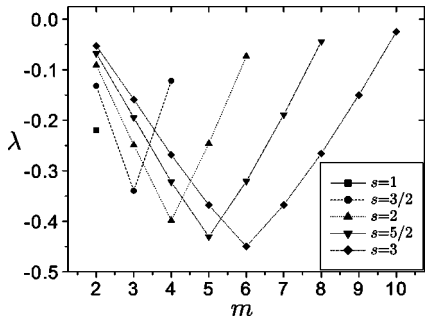

FIG. 5. Growth rates of the fastest splitting modes with the angular eigenvalue m for different winding numbers. The splitting into $1/2$ defects ($m=2s$) is always the fastest.

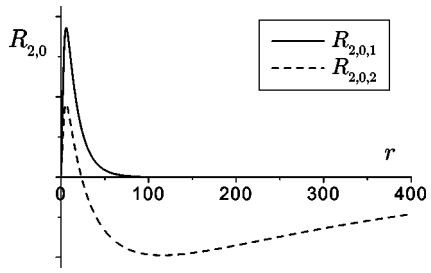

FIG. 6. Radial eigenfunctions of the first two growing modes (not normalized), responsible for the escape of the ±1 defect ($m=0$). These modes are quite extensive, yet localized [Eq. (33)]; the range of the second function is $\approx 1000\xi$.

discrete spectrum for all the modes x_2, Figs. 6 and 7. The modes x_{-2} are decaying, as are all the other modes with $n \neq 0$. According to Eq. (22), for half-integer winding numbers the lowest angular eigenvalue is $n=1/2$—these defects are stable with respect to the escape.

Noting that $g_2(r \gg \xi) \to 0$ and $g_{-2}(r \gg \xi) \to g_{-2}(\infty) > 0$, the asymptotic behavior for $n=0$ is

$$R_{2,0} \propto r^{-1/2} e^{\pm\sqrt{-\lambda}r}, \tag{33}$$

i.e., the functions $R_{2,0}$ are localized. It turns out that here the localized modes are much more extensive than in the case of the splitting. One may think there is little point in studying the splitting if the defects are always unstable to the escape. There exist, however, a large difference in growth rates of the two types of unstable modes, connected with the large difference in localization, Eq. (33). In the case of the ±1 defect, in the one elastic constant approximation the splitting is approximately 53-times faster than the escape. Whence, provided we prepared the ±1 configuration, it would always split before it could even start escaping. Of course, it is just due to the fast splitting that the initial configuration is very hard to prepare, even numerically.

VI. PERTURBATION ANALYSIS

We are interested in the changes of the ground state and its stability upon subjecting our system to a small perturbation, e.g., weak external field. We make a first order perturbation analysis, keeping the perturbation general. Let us denote the nonlinear time evolution operator (9) by $\mathcal{O}$,

$$\mathcal{O}(\mathbf{q}) = \dot{\mathbf{q}}, \quad \mathcal{O}(\mathbf{a}) = \mathbf{0}, \tag{34}$$

where $\mathbf{a}$ is the ground state components. Defining the linearized operator $\mathcal{L}$,

$$\left.\frac{\partial \mathcal{O}}{\partial \mathbf{q}}\right|_{\mathbf{a}} = \mathcal{L}, \tag{35}$$

where $\mathcal{L}=\mathcal{L}(\mathbf{a})$ depends on the ground state, the eigensystem evolving from the system (15)–(19) can be written as

$$\mathcal{L}\mathbf{x} = \dot{\mathbf{x}} = -\lambda\mathbf{x}. \tag{36}$$

Introducing a perturbation operator $\mathcal{P}$, nonlinear in general,

$$\mathcal{O}' = \mathcal{O} + \epsilon\mathcal{P}, \tag{37}$$

the time evolution of $\Delta\mathbf{q}$ in the vicinity of the ground state $\mathbf{a}$ is

$$\Delta\dot{\mathbf{q}} = \mathcal{O}(\mathbf{a}+\Delta\mathbf{q}) + \epsilon\mathcal{P}(\mathbf{a}+\Delta\mathbf{q}), \tag{38}$$

which to the first order in ϵ reads:

$$\Delta\dot{\mathbf{q}} = \mathcal{L}\Delta\mathbf{q} + \epsilon\mathcal{P}(\mathbf{a}). \tag{39}$$

Requiring $\Delta\dot{\mathbf{q}}=0$, the correction $\Delta\mathbf{q} \equiv \Delta\mathbf{a}$ of the ground state $\mathbf{a}$ is obtained, formally:

$$\Delta\mathbf{a} = -\epsilon\mathcal{L}^{-1}\mathcal{P}(\mathbf{a}). \tag{40}$$

Adopting the bracket notation and expressing the functions $\Delta\mathbf{q}$ and $\mathcal{P}(\mathbf{a})$ in terms of the normalized eigenstates $|\mathbf{x}_i\rangle$ of $\mathcal{L}$ [Eq. (36)], $\Delta\mathbf{q}=\Sigma_i c_i(t)|\mathbf{x}_i\rangle$, $\mathcal{P}(\mathbf{a})=\Sigma_i P_i|\mathbf{x}_i\rangle$, Eq. (39) becomes

$$\dot{c}_i = -\lambda_i c_i + \epsilon P_i, \quad P_i = \langle \mathbf{x}_i|\mathcal{P}(\mathbf{a})\rangle. \tag{41}$$

The solution for the initial condition $c_i(0)=0$ is

$$c_i(t) = \epsilon\frac{P_i}{\lambda_i}[1-\exp(-\lambda_i t)], \tag{42}$$

furnishing the time evolution of the ground state when the perturbation $\mathcal{P}$ is turned on at $t=0$. In the case when $\lambda_i>0$ for all i with a nonzero P_i, the time evolution leads to the corrected ground state (40). For $\lambda_i=0$ and $P_i\neq 0$ the linear perturbation analysis cannot be applied. If $\lambda_i<0$ (i.e., $\mathbf{a}$ is unstable) and $P_i\neq 0$, however, the system never reaches the corrected ground state but is driven away from it exponentially as the perturbation triggers a growing mode.

If $\lambda_i>0$ for all i with a nonzero P_i, one can determine the first order correction of the eigenvalue using the unperturbed eigenmodes. Linearization of the perturbed operator (37) around the corrected ground state $\mathbf{a}'=\mathbf{a}+\Delta\mathbf{a}$, where $\mathcal{O}'(\mathbf{a}')=0$, gives

$$\mathcal{O}'(\mathbf{a}'+\mathbf{x}) = \left(\mathcal{L} + \left.\frac{\partial\mathcal{L}}{\partial q_i}\right|_{\mathbf{a}}\Delta a_i + \epsilon\left.\frac{\partial\mathcal{P}}{\partial\mathbf{q}}\right|_{\mathbf{a}}\right)|\mathbf{x}\rangle \equiv (\mathcal{L}+\Delta\mathcal{L})|\mathbf{x}\rangle, \tag{43}$$

where $\Delta\mathbf{a}$ is given by Eq. (40) and is first order in ϵ. The second term in Eq. (43) is the consequence of the nonlinear-

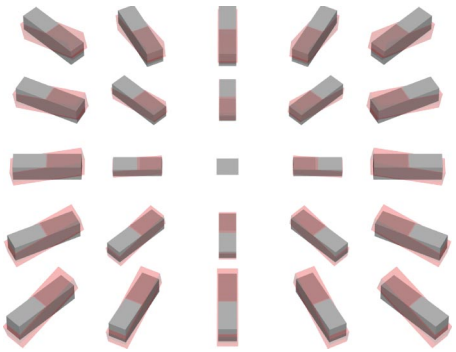

FIG. 7. (Color online) Cross section through the $s=1$ radial disclination line: the ground state (gray/dark) is perturbed by the escape mode (red/light). The mode is quite extensive, only the very central part is depicted here (before the maximum of $R_{2,0,1}$ in Fig. 6) to point out the vanishing perturbation in the center.

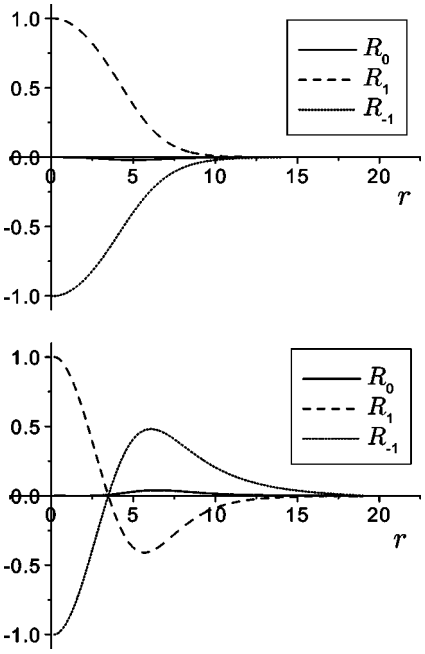

FIG. 8. Radial eigenfunctions of the splitting modes with $m=4$ for the $s=2$ defect: (a) $\lambda=-0.40$ and (b) $\lambda=-0.059$.

ity of $\mathcal{O}$ and represents a perturbation of the linearized operator due to the corrected ground state. It does not appear in the standard perturbation theory of a linear operator, e.g., the Hamiltonian in quantum mechanics. Requiring

$$\langle \mathbf{x}_i|\mathcal{L}+\Delta\mathcal{L}|\mathbf{x}_i\rangle = -\lambda_i'\langle \mathbf{x}_i|\mathbf{x}_i\rangle, \tag{44}$$

the corrected eigenvalue $-\lambda_i'$ is

$$-\lambda_i' = -\lambda_i + \langle \mathbf{x}_i|\Delta\mathcal{L}|\mathbf{x}_i\rangle. \tag{45}$$

In the following, we illustrate the results of the perturbation analysis with three particular examples.

A. Computational grid-reduced symmetry

We address an important point concerning the numerical simulation of defects with strengths higher than 1/2, e.g., when studying the splitting numerically. The discretization on a square grid (C_4 symmetry) standardly used in simulations introduces an artifactual perturbation with the C_4 symmetry,

$$\mathcal{P} = \sum_{n=0,1,2,3,\ldots} P_{4n}(r)\cos(4n\phi). \tag{46}$$

If the spectrum contains a growing mode with $m=4n$, according to Eq. (42) it will experience a boost upon "turning on" the perturbation—the mode will grow at a nonvanishing rate despite its initial amplitude of zero and will overwhelm other possibly faster modes. An example of such splitting is shown in Figs. 8 and 9. Thus on the square grid it is possible to simulate defects not possessing such modes, i.e., those with strengths $\pm 1/2$ and ± 1 only. If the grid were rectangular (C_2 symmetry), only the $\pm 1/2$ defect would remain. One must bear this in mind when trying to study the splitting numerically.

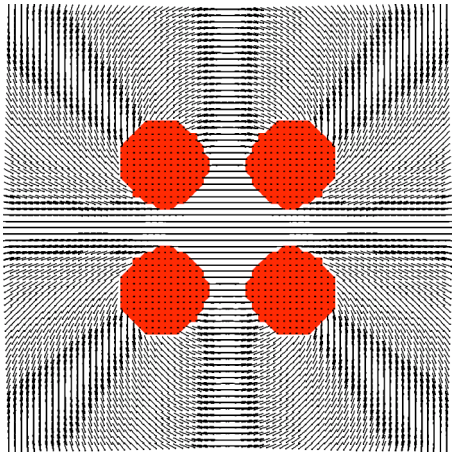

FIG. 9. Splitting of the $s=2$ defect into four 1/2 defects, $m=4$; the corresponding radial eigenfunctions are depicted in Fig. 8. The $m=4$ modes are numerically boosted due to the C_4 symmetry of the computational grid.

In an alternate inference one can ask why a mode not possessing the C_4 symmetry experiences no boost. In this case, the rotations of C_4 generate at least two different modes, as opposed to the identity representation in the previous case. These are degenerated with respect to their placement on the grid since the grid is invariant to C_4. Therefore in a pure ground state neither must be favored and hence at vanishing amplitude their growth rate must vanish.

B. Selecting the splitting channel

Equation (42) suggests that by applying a perturbation with a particular angular symmetry one could favor the corresponding splitting channel. Perhaps the simplest perturbation to realize is a homogeneous electric field applied perpendicularly to the disclination line. In the electric field $\mathbf{E}$, the perturbation is (in Cartesian notation)

$$\mathcal{P} = \frac{1}{3}(E_iE_j - E^2\delta_{ij}/3), \tag{47}$$

where $E \quad E/E_0$ and $E_0=\sqrt{L/\varepsilon_0|\varepsilon_a|}/\xi$ is the field with the coherence length equal to ξ. Putting $\mathbf{E}=E\hat{\mathbf{e}}_x$ and using the tensorial base (3), one gets

$$\mathcal{P} = \begin{Bmatrix} \mathcal{P}^{(0)} \\ \mathcal{P}^{(1)} \\ \mathcal{P}^{(-1)} \end{Bmatrix} = \frac{1}{3}E^2 \begin{Bmatrix} -1/\sqrt{6} \\ \cos(2\psi_0+2s\phi)/\sqrt{2} \\ -\sin(2\psi_0+2s\phi)/\sqrt{2} \end{Bmatrix}. \tag{48}$$

According to Eq. (42), such a perturbation triggers the mode with $m=2s$ (besides, it breaks the angular degeneracy), i.e., the mode responsible for the splitting into 1/2 defects which is already the fastest and thus dominating. To favor alternative splitting channels one should therefore look for perturbations with different symmetry. Staying within electric field effects, the optical tweezer seems to be a good candidate [15,16]. In a single beam optical trap polarized in the direction of the disclination line, for example, the perturbation would be of the form

$$\mathcal{P}^{(0)} = \frac{1}{3}\sqrt{\frac{2}{3}}E^2 \sum_n c_{2n}(r)\cos(2n\phi), \tag{49}$$

thus coupling to modes with $m=2n$ symmetry. However, it is fair to emphasize that the angular dependence must be present in the region where the growing mode is nonzero or the scalar product in Eq. (41) will vanish, i.e., c_{2n} for $n \neq 0$ should not vanish all down to the 100 nm scale, which is hard to achieve by optical means.

The perturbation (48) not only triggers the $m=2s$ mode but also breaks its angular degeneracy, i.e., the splitting "direction" depends on the relative orientation of the electric field and the defect (given by ψ_0). It is worth mentioning that in case there exist no splitting modes, i.e., for $|s|=1/2$, the perturbation (48) removes the angular degeneracy of the fluctuations and the splitting of the relaxation rate can be calculated from Eq. (45).

C. Field-suppressed escape

In the case of $\varepsilon_a < 0$, the escape of the disclination can be suppressed by an (homogeneous) electric field oriented along the disclination line not triggering the spliting modes. Performing the perturbation analysis, we can make an estimate of the required field strength. The perturbation is now

$$\mathcal{P}^{(0)} = -\frac{1}{3}\sqrt{\frac{2}{3}}E^2. \tag{50}$$

According to Eq. (45), one must provide the corrected ground state $\Delta\mathbf{a}$ given by Eq. (40) or Eq. (42) and require $\lambda' = 0$ for the largest in absolute eigenvalue. The ground state correction involves the tensor components 0 and 1:

$$|\Delta\mathbf{a}\rangle = -\frac{1}{3}\sqrt{\frac{2}{3}}E^2 \sum_n \frac{\int r dr R_{0,0,n}(r)}{\lambda_n} \begin{vmatrix} x^{(0)}_{n,m=0} \\ \\ x^{(1)}_{n,m=0} \end{vmatrix}, \tag{51}$$

where $R_{0,0,n}$ is the $m=0$ radial eigenfunction of the zeroth tensor component corresponding to λ_n. Note that the corrected ground state is well defined, i.e., none of the λ's in Eq. (51) are zero, and there is also no boost as the growing modes all have $m \neq 0$. From Eq. (45) we get

$$\lambda = \frac{1}{3}\sqrt{\frac{2}{3}}E^2 \sum_{i=0,1} \left[\left. \frac{\partial g_2}{\partial q_i} \right|_{\mathbf{a}} \langle x^{(2)}_{m=0} | \Delta a^{(i)}(r) | x^{(2)}_{m=0} \rangle \right], \tag{52}$$

where $|x^{(2)}_{m=0}\rangle \propto R_{2,0}(r)\mathbf{T}_2$ is the growing mode corresponding to the most negative λ. Equation (52) determines the electric field strength E required to stabilize the disclination (in an infinite system) against the escape. As its evaluation inevitably involves numerics, it is perhaps more convenient to determine the field strength by a direct numeric calculation, yielding $E=0.086$ (corresponding to the coherence length of 12ξ) in the one elastic constant approximation.

VII. ELASTIC ANISOTROPY

The eigenmode problem was solved semianalytically in the one elastic constant approximation. Beyond this approximation, one has to include more elastic terms in the free-energy density (1): up to the third order in $\mathbf{Q}$, quadratic in the first derivative, and omitting surface terms these are

$$f = \frac{1}{2}L(\partial_i \mathbf{Q}_{jk})^2 + \frac{1}{2}L'(\partial_i \mathbf{Q}_{ik})(\partial_j \mathbf{Q}_{jk}) + \frac{1}{2}L''\mathbf{Q}_{ij}(\partial_i \mathbf{Q}_{kl})(\partial_j \mathbf{Q}_{kl}), \tag{53}$$

which is the minimum set of elastic terms to distinguish between splay (K_{11}), twist (K_{22}), and bend (K_{33}) distortions:

$$K_{11} = \frac{9S^2}{4}(2L + L' - SL''), \tag{54}$$

$$K_{22} = \frac{9S^2}{4}(2L - SL''), \tag{55}$$

$$K_{33} = \frac{9S^2}{4}(2L + L' + SL''). \tag{56}$$

Including any of the new elastic terms, the generalized cylindrical symmetry of the ground state is lost, making the eigenmode problem two-dimensional, i.e., the variables r and ϕ cannot be separated any longer. It is only in the case of the $+\mathbf{1}$ disclination with $\psi_0=0$ or $\psi_0=\pi/2$ (radial and circular disclinations) that the cylindrical symmetry is retained, so that without the third-order term the separation would still be possible. The third-order term, however, brings about mixed derivatives, which inevitably prevent the separation.

Nevertheless, one is interested in whether the elastic anisotropy could cause a metastability of the disclination core with respect to the splitting. For the ± 1 disclinations this can be easily examined numerically using realistic elastic parameters. The answer is rather surprising: moderate elastic anisotropy, e.g., in thermotropic liquid crystals like 5CB or MBBA, gives no metastability. It is only in the extreme cases that the core could become metastable against the splitting [17].

VIII. SUMMARY

Resorting to the one elastic constant approximation we have solved the complete tensor fluctuation problem of the nematic disclination line with a general winding number. We found no metastability, i.e., we were able to find growing fluctuation modes leading to the splitting and decay, respectively. Several splitting modes characterized by their angular symmetry were found to exist, each yielding a particular splitting channel. The possibility of selecting these channels was discussed.

It must be emphasized that the splitting instability is always there and cannot be affected by any confinement, unless it were in the (nonrealistic) nanometer region. Conversely, the confinement can stabilize the disclination with respect to the escape, as in this case the growing modes are much more extensive, while it is known that also the elastic anisotropy (in connection with the confinement) favors/disfavors the escape in the third dimension [14,1].

Numerically we found, rather surprisingly, that a moderate elastic anisotropy does not introduce any metastability with respect to the splitting or escape (in the latter case for an unconfined system). In the case of a severe anisotropy, e.g., close to the SmA phase, the situation changes and will be reported elsewhere.

ACKNOWLEDGMENTS

Many thanks to M. Praprotnik [18], A. Kodre, and G. Veble. This work was supported by the Slovenian Office of Science (Program P1-0099) and U.S.-Slovene NSF Joint Found (Grant No. 9815313).

[1] R. B. Meyer, Philos. Mag. **27**, 405 (1973).
[2] N. Schopohl and T. J. Sluckin, Phys. Rev. Lett. **59**, 2582 (1987).
[3] E. Penzenstadler and H.-R. Trebin, J. Phys. (France) **50**, 1027 (1989).
[4] A. Sonnet, A. Kilian, and S. Hess, Phys. Rev. E **52**, 718 (1995).
[5] P. E. Cladis, Philos. Mag. **29**, 641 (1974).
[6] S. Hess, Z. Naturforsch. A **30A**, 728 (1975).
[7] V. L. Pokrovskii and E. I. Kats, Zh. Eksp. Teor. Fiz. **73**, 774 (1977) [Sov. Phys. JETP **46**, 405 (1977)].
[8] T. Qian and P. Sheng, Phys. Rev. E **58**, 7475 (1998).
[9] W. H. Press, B. P. Flannery, S. A. Teukolsky, and W. T. Vetterling, *Numerical Recipes* (Cambridge University Press, Cambridge, England, 1986).
[10] D. Svenšek and S. Žumer, Phys. Rev. E **70**, 040701(R) (2004).
[11] A. Mertelj and M. Čopič, Phys. Rev. E **69**, 021711 (2004).
[12] D. Svenšek and S. Žumer, Phys. Rev. E **66**, 021712 (2002).
[13] H. Pleiner, M. Liu, and H. R. Brand, Rheol. Acta **41**, 375 (2002).
[14] P. Cladis and M. Kléman, J. Phys. (France) **33**, 591 (1972).
[15] M. Yada, J. Yamamoto, and H. Yokoyama, Phys. Rev. Lett. **92**, 185501 (2004).
[16] I. Musevic, M. Skarabot, D. Babic, N. Osterman, I. Poberaj, V. Nazarenko, and A. Nych, Phys. Rev. Lett. **93**, 187801 (2004).
[17] D. Svenšek, P. Ziherl, and S. Žumer (unpublished).
[18] D. Janežič and M. Praprotnik, Int. J. Quantum Chem. **84**, 15 (2001).